Arc-Polarized, Nonlinear Alfvén Waves and Rotational Discontinuities: Directions of Propagation?

Bruce '1'. Tsurutani
Christ ian M. Ho
Regina Sakurai
John K. Arballo
Jet l'repulsion Laboratory
California Institute of Technology
4800 Oak Grove Drive
Pasadena, CA 91109

Peter Riley*
Lunar and Planetary Laboratory
University of Arizona, Tucson, AZ 85721

and

Andre Balogh
Imperial College of Science & Technology
The Blackett Laboratory
Prince Consort Road
1 ,01)(1[)11, SW7 2BZ England

* Now at Los Alamos National laboratory,
Los Alamos, New Mexico

()/? ()/9()

A 3STRACT

Large amplitude, noncompressive Alfvén waves and rotational discontinuities are shown to be "arc-polarized" The slowly rotating Alfvén wave portion plus the fast rotating discontinuity comprise 360° n phase rotation. The nagnetic field vector perturbation ies in a plane. There are wo (or more) possible interpretations to the observations. The first is that the waves are plane polarized, and are propagating in the minimum variance direction. With this interpretation, the waves would be propagating at substantial angles to $\vec{B}_0$ and would consist of both right-hand and left-hand polarized components. We discuss several significant problems with this interpretation. A second interpretation is that the waves are spherical rather than planar. The arc-polarization can be thought of as a large amplitude extension of linearly polarized waves. Thus, this interpretation is that these Alfvén waves and discontinuities are spherical waves which are arc-polarized, or stated more succinctly, they are arc-polarized spherical waves. If this is correct hen the direction of wave propagation $\hat{k}$ is in the intermediate variance direction

INTRODUCTION

It has already been theoretically argued that nonlinear Alfvén waves cannot be plane polarized (Barnes, 1976). For large-amplitude waves ir which the magnetic field magnitude is conserved, the field perturbation vector rotates on the surface of a sphere (Goldstein et al., 974). Goldstein et al. (974) further pointed ou that "the direction of propagation of these [large amplitude] waves, cannot be determined by looking for minimum in a variance matrix constructed from observed field fluctuations". Barnes (198) and Tsurutani et al. (1993) have demonstrated hat even for small amplitude waves, minimum variance analyses of intervals containing many waves or many wave cycles might be meaningless. There can be significant errors in both in the direction of propagation and/or in wave polarization. Only single wave cycle analyses can ead to meaningful results, even for waves with small amplitudes

Recently, Jlysses results (Tsurutani et al., 994, 1996; Smith et al., 1995a, b; Balogh et al., 995; Iorbury et al., 995) have indicated the presence of large amplitude, $|\Delta\vec{B}|/|B| \sim 1$–$2$, Alfvén waves within high-speed streams emanating from coronal holes (Phillips et al., 995a, b). The Alfvén waves are often phase-steepened, with rotational discontinuities (RDs) bounding the edges (Tsurutani et al. 1994; 1995a; 1996). The nonlinear Alfvén waves and RDs are typically arc-polarized (Tsurutani et al., 1994; 1995a; 1996; Riley et al., 1995; 1996).

The purpose of this paper is to examine the field and plasma data for nonlinear arc-polarized Alfvén waves and rotational discontinuities to explore the applicability or nonapplicability of the Principal Axis (PA) technique of Sonnerup and Cahill (1967). We will argue that the Principal Axis (PA) technique is applicable for finding the wave direction of propagation for arc-polarized waves. However, we will argue that wave propagation direction $\hat{k}$ is not in the minimum variance direction, but lies along the intermediate variance direction.

METHOD OF ANALYSIS

The covariance of the cross products of the three orthogonal components of the magnetic field are diagonalized, giving three eigenvalues (λ_1, λ_2, λ_3), corresponding to the maximum, intermediate and minimum variance directions, respectively. We will call the corresponding eigenvectors $\vec{k}_1, \vec{k}_2, \vec{k}_3$. The direction of minimum variance, $\hat{k}_3$, gives the normals to surfaces such as tangential discontinuities. It also gives the direction of propagation $\hat{k}$ for circularly or elliptically polarized electromagnetic waves (Smith and Tsurutani, 1976). We will apply this general method of analysis for the analysis of arc-polarized Alfvén waves and rotational discontinuities and comment on the interpretation of the results.

RESULTS

Figure 1 shows an example of a magnetic field discontinuity at ~00 58 UT, August 6, 1995. The Ulysses spacecraft was at a heliographic latitude +80.5° and a distance 2.0 AU from the sun. The top panel shows the field component in the minimum variance coordinate system as described previously. The magnetic field magnitude panel shows that the magnetic field magnitude is conserved across the discontinuity. The field is primarily along the $\hat{B}_2$ direction and is almost zero along $\hat{B}_3$. Similar discontinuities were observed by Neugebauer (1989).

The bottom panel in Figure 1 gives the hodogram for the discontinuity in the B_1 - B_2 plane. By definition, the majority of the vector perturbation is in the B_1 direction and less perturbation in the B_2 direction ($\lambda_1/\lambda_2 \approx 28$). The perturbation vector sweeps out an "arc " in the hodogram. The variation in the B_3 direction is less than in the B_2 direction, as the ratio λ_2/λ_3 = 2.6 indicates. The angle between $\hat{k}_3$ and $\vec{B}_0$ is 89°. The angle between $\hat{k}_2$ and $\vec{B}_0$ is 12", a point that we will return to later.

Figure 2a illustrates a rotation in the ambient magnetic field on July 29, 1995. Ulysses was again over the north heliographic pole at approximately the same distance as the previous example. The field variation is again illustrated in the minimum variance coordinate system. The field magnitude is constant, to first order. The field is primarily in the $\hat{k}_2$ direction and is small in the $\hat{k}_3$ component.

Figure 2b gives the hodogram for the points 1-3 interval (see the Figure) in the B, -112 plane. The perturbation starts at point " 1 " and ends at point "3". From point "l" to "2" the field rotates slowly, and from point "2" to point "3" the rotation is much more rapid (the latter interval includes the rotational discontinuity). The rotation is originally from left to right and then back to the left again. This is the relationship of an Alfvén wave and a rotational discontinuity discussed in Tsurutani et al. (1994). The rotational discontinuity and "wave" together form a 360° rotation in phase. Thus the rotational discontinuity can be interpreted as the phase-steepened edge of an Alfvén wave. λ_1/λ_2 is ~4.5 and $\lambda_2/\lambda_3 \approx 3.8$. The angle of $\hat{k}_3$ relative to $\vec{B}_0$ is 77° and the angle of $\hat{k}_2$ relative to $\vec{B}_0$ is 13°.

For both examples shown (Figures 1 and 2), the perturbation vector rotates in a plane. This is shown by the large ratios of λ_2/λ_3, 2.6 and 3.8, respectively. Thus, one possible interpretation is that these arc-polarized waves are propagating along the $\hat{k}_3$ direction. In these two cases θ_{kB} would thus be 89° and 72", respectively. Such highly oblique angles Of propagation seemingly would be peculiar. Also for the latter case (Figure 2), this interpretation would imply that the slow rotational part and fast rotational part of the wave would correspond to a left-hand polarized (Alfvénic) portion and right-hand polarized (magnetosonic) portion, assuming propagation away from the sun (if propagating towards the sun, the sense of rotation would be reversed). Since the phase speeds of left-hand waves and right-hand waves are considerably different (the right-hand branch has higher phase-speeds), one would expect the right-hand portion to quickly pull away. The "wave" could not stay intact.

There are other problems with the interpretation that $\hat{k}_3$ defines the direction 01 propagation of the arc-polarized wave. The magnetosonic portion should be compressive. especially if it is propagating nearly orthogonal to $\vec{B}_0$. '1'here. is no evidence for this in the data. in fact, the field magnitude in the fast rotational portion is slightly less than in the slow rotational portion. Another problem is that the slowly rotating portion dots not always have only one sense 01' "polarization". In the example shown in Tsurutani et al. (1 994), the slow rotating portion covered about 270" in phase rotation (not shown). '1'bus, for this case, the slow rotation consisted of both left-hand and right-hand polarized parts. This corresponds to "angular overshoots" discussed in Neugebauer (1989). Again, the "wave" would quickly separate into two parts.

DO ARC-POLARIZED WAVES PROPAGATE IN THE $\hat{k}_2$ DIRECTION'?

To explore the meaning of the principal axis results for arc-polarized RDs and Alfvén waves, we show a schematic for both linear and nonlinear Alfvén waves (rotational] discontinuities are high frequency Alfvén waves) in Figure 3. At the top, a small amplitude Alfvén wave train is schematically shown (taken after Alfvén, 1950). The wave amplitudes arc small (±1nT) in comparison to the ambient field strength of 10 nT, so the waves arc essentially "linear" in this case. The waves are transverse and noncompressive. The waves arc propagating in the + or - x-direction. This is the standard one-dimensional Alfvén "wave train" shown in many textbooks.

The direction of maximum variance is along the z-axis. The minimum variance is the $\hat{x}$ - $\hat{y}$ plane. For this case $\lambda_2 = \lambda_3 = 0$. However, because the wave is linearly polarized, the direction of $\vec{k}$ can only be localized to the plane perpendicular to λ_1 by the minimum variance technique. The MV technique does not give a unique solution for this case.

Figure 3b is a similar case, but for a wave with much larger amplitude. The wave is again noncompressive and therefore must now be "arc-polarized" to maintain constant |B|. The tip of the magnetic perturbation vector rotates on the surface of a sphere (Goldstein et al., 1974). Although the dominant perturbation is still in the $\hat{z}$ direction, there are now perturbations in the ~-direction as well. A Principal Axis Analysis would show that the maximum variance is along $\hat{z}$, intermediate variance in the $\hat{x}$-direction, and the minimum variance in the $\hat{y}$-direction as illustrated in the Figure. Note that the perturbation vector lies in a plane ($\hat{x}-\hat{z}$), similar to the data examples of Figures 1 and 2. We have already given arguments why it is difficult to imagine that the wave is propagating in the y-direction. A simpler explanation is that the wave is propagating in the $\hat{x}$ direction. As the linearly polarized waves grow in amplitude from a linear to nonlinear state (from 3a to 3b), in order to maintain incompressibility, they gradually evolve into arc-polarized states. in this scenario, the wave polarization does not consist of a left-hand and a right-hand component at all, but the entire 360° phase cycle is "arc-polarized". Also in this interpretation the waves are not plane-polarized. The waves are a special case of spherical waves (the perturbation vector rotates on the surface of a sphere). Thus, a more definitive label would be "arc-polarized spherical waves".

Panel 3c) shows the relevant wave perturbation vectors. For the case where the wave magnetic field perturbation $\vec{B}_w$ is in the $+\hat{z}$ direction, as seen in the previous data examples, the $\vec{V}_w$ perturbation is in the same direction. The wave electric field, $\vec{E}_w$, is given by

$$\vec{E}_w = \frac{-\vec{V}_w \times \vec{B}_o}{c} \qquad (1)$$

Thus, $\vec{E}_w$ is in the $-\hat{y}$ direction. The Poynting vector or direction of wave energy is given by:

$$\vec{k} = \vec{E}_w \times \vec{B}_w \qquad (2)$$

From the schematic, it is noted that this is along the $\hat{x}$ axis, or along the ambient magnetic field. This sense is the same as that for small amplitude waves shown in 3a. Note that the direction of wave energy is along $\hat{k}_2$ or the intermediate variance direction.

Figures 4a and 4b show the results of principal axis analyses of 40 spherical arc-polarized Alfvén wave events and 63 noncompressional ($\Delta|B|/|B| \leq 0.2$) directional discontinuities (DDs) with arc polarization. The discontinuity set consisted of all clear arc-polarized events that occurred within a single day. The top panel gives the number of events over 10° angular bins of $\hat{k}_2$ relative to $\vec{B}_0$. For the slowly rotating Alfvén waves, the greatest number of events occur at large $\theta_{k_2B_0}$ angles. The discontinuities have a broad range of angles between k_2 and B_0. However, when the number of cases are normalized by taking the solid angle subtended into account, we get the bottom two panels. From these normalized distributions, it is found that Alfvén waves and the arc-polarized discontinuities are primarily directed along the ambient magnetic field. 'Ibis is consistent with the results obtained in the ecliptic plane (Belcher and Davis, 1971), at high latitudes (Smith et al., 1995b), and here using analyses involving $\vec{V}_{sw}$ and $\vec{B}_0$.

CONCLUSIONS

For circularly polarized or elliptically polarized electromagnetic waves, $\hat{k}_3$ gives the correct wave direction of propagation (Smith and Tsurutani, 1976). For small amplitude linearly polarized electromagnetic waves, there is a 360° ambiguity, and therefore $\hat{k}$ cannot be determined from the MV method alone, However, as the noncompressive linearly polarized waves become larger in amplitude, the "arc" removes the ambiguity from principal axis analysis results such that the wave $\dot{k}$ can be determined. One possible interpretation is that the waves are spherical waves with arc-polarization and that the wave $\ddot{k}$ is along the intermediate variance direction.

Acknowledgments. Portions of this work were performed at the Jet l'repulsion Laboratory, California Institute of Technology, Pasadena, under contract with the National Aeronautics and Space Administration.

REFERENCES

Alfvén, H., Cosmical Electrodynamics, Oxford Univ. Press, New York, 1980.

Balogh, A., E. J. Smith, B. T. Tsurutani, et al., The heliospheric magnetic field over the southern polar region of the Sun, Science 268, 945, 1995.

Barnes, A., On the nonexistence of plane-polarized large amplitude Alfvén waves, J. Geophys. Res., 81, 281, 1976.

Barnes, A., Interplanetary Alfvénic fluctuations: A stochastic model, J. Geophys. Res., 86, 7498, 1981.

Belcher, J. W. and L. Davis, jr., Large amplitude Alfvén waves in the interplanetary medium, 2, J. Geophys. Res., 76, 3534, 1971.

Goldstein, M. L., A. J. Klimas and F. D. Barish, On the theory of large amplitude Alfvén waves, Solar Wind Three, edited by C. T. Russell, IGPP, UCLA, 385, 1974.

Horbury, T. S., A. Balogh, R. J. Forsyth and E. J. Smith, Anisotropy of inertial range turbulence in the polar heliospheric, Geophys. Res. Lett., 22, 3405, 1995.

Neugebauer, M., The structure of rotational discontinuities, Geophys. Res. Lett., 16, 1261, 1989.

Phillips, J. L., S. J. Bame, W . C. Feldman, et al., Ulysses solar wind plasma observations at high southerly latitudes Science 268, 1030," I 995a.

Phil lips, J. L., S. J. Bame, A. names et al., Ulysses solar wind plasma observations from pole to pole, Geophys. Res. Lett., 22, 3301, 1 995b.

Riley, 1'., C. P. Sonnett, A. Balogh et a]., Alfvénic fluctuations in the solar wind: A case study using Ulysses measurement, Space Xi. Rev., 72, 197, 1995.

Riley, P., C. P. Sonnett, B. T. Tsurutani et al., The properties of arc-polarized Alfvén waves in the ecliptic plane: Ulysses observations, submitted to J. Geophys. Res., 1996.

Smith, E. J., and B. T. Tsurutani, Magnetosheath lion roars, J. Geophys. Res., 81, 2261, 1976.

Smith, E. J., M. Neugebauer, A. Balogh, et al., Ulysses observations of latitude gradients in the heliospheric magnetic field: Radial components and variances, Space Sci. Rev., 72, 166, 1995a.

Smith, E. J., A. Balogh, M. Neugebauer and D. J. McComas, Ulysses observations of Alfvén waves in the southern and northern solar hemispheres, Geophys. Res. Lett., 22, 3381, 1995b.

Sonnerup, B. U. O. and 1,. J. Cahill Jr., Magnetopause structures and altitude from Explorer 12 observat ions, J. Geophys. Res., 72, 171, 1 ')67.

Tsurutani, B. 'I'., D. J, Southwood, E. J. Smith, et al., A survey of low frequency waves at Jupiter: The Ulysses encounter, J. Geophys. Res., 98, 21203, 1993.

Tsurutani, B. '1'., C. M. Ho, E. J, Smith, et al., The relationship between interplanetary discontinuities and Al fvén waves: Ulysses observations, Geophys. Res. Lett., 2 1, 2267, 1994.

Tsurutani, B. 'I'., E. J. Smith and C. Ho et al., Interplanetary discontinuities and Al fvén waves, Space Sci. Rev., 2.2, 205, 1995:1.

Tsurutani, B. T., C. M. Ho, J. K. Arballo, et al., Interplanetary discontinuities and Alfvén waves at high heliographic latitudes: Ulysses, J. Geophys. Res., 101, 11027, 1996.

Figure Captions

Figure 1. A magnetic field discontinuity at +80° latitude, and 2.0 AU from the sun. The discontinuity is arc-polarized.

Figure 2. An arc-polarized Alfvén wave plus arc polarized rotational discontinuity. The two perturbations are nearly coplanar.

Figure 3. A schematic for small amplitude linearly polarized Alfvén waves (top) and large amplitude arc-polarized Alfvén waves (bottom).

Figure 4. The angle between the intermediate variance direction and $\vec{B}_0$ for 40 arc-polarized Alfvén waves and 63 arc-polarized discontinuities (top panels). The bottom panels are the data in the top panels normalized by solid angle.

Ulysses **August 6, 1995**
Day 218

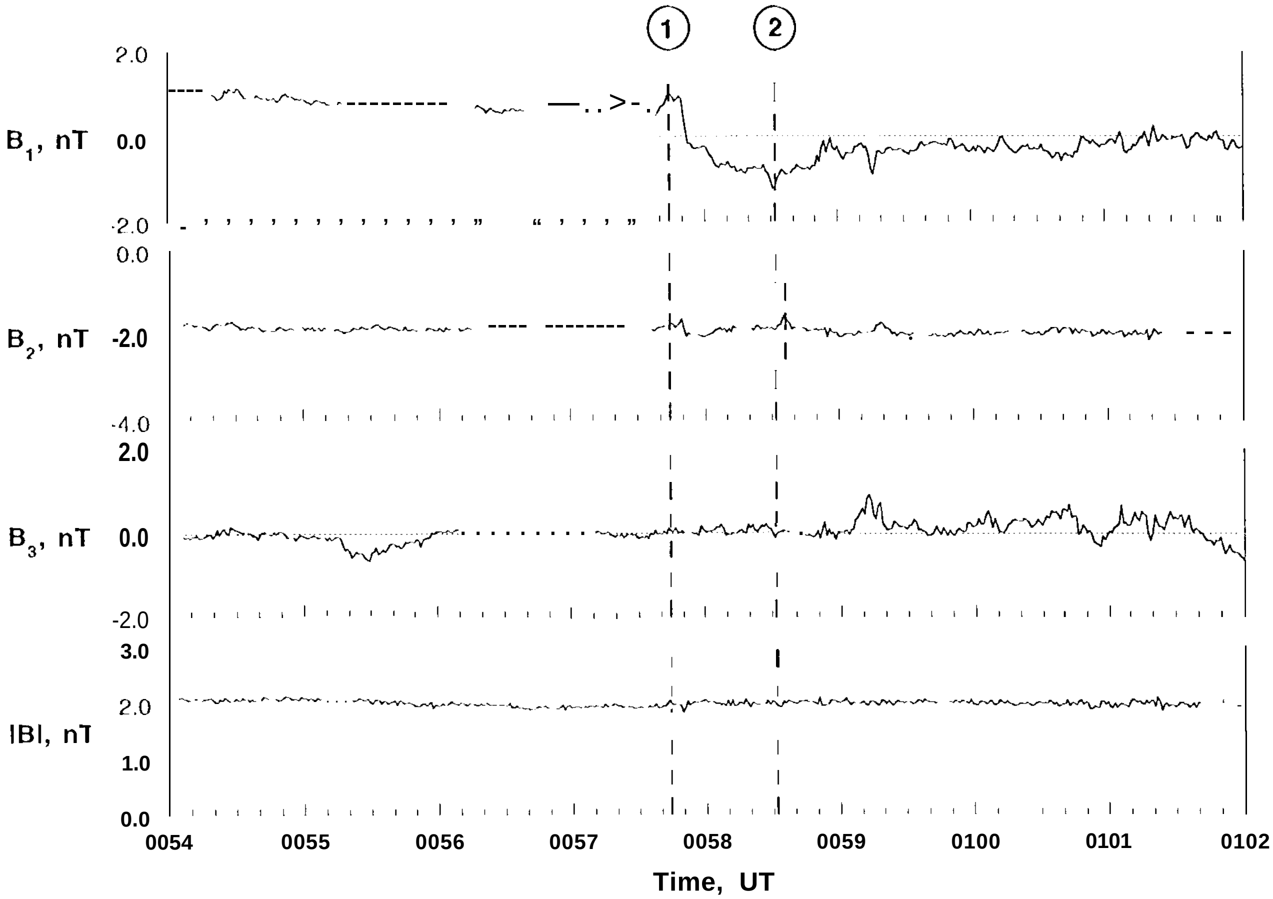

Ulysses Heliographic Latitude = 80.05”

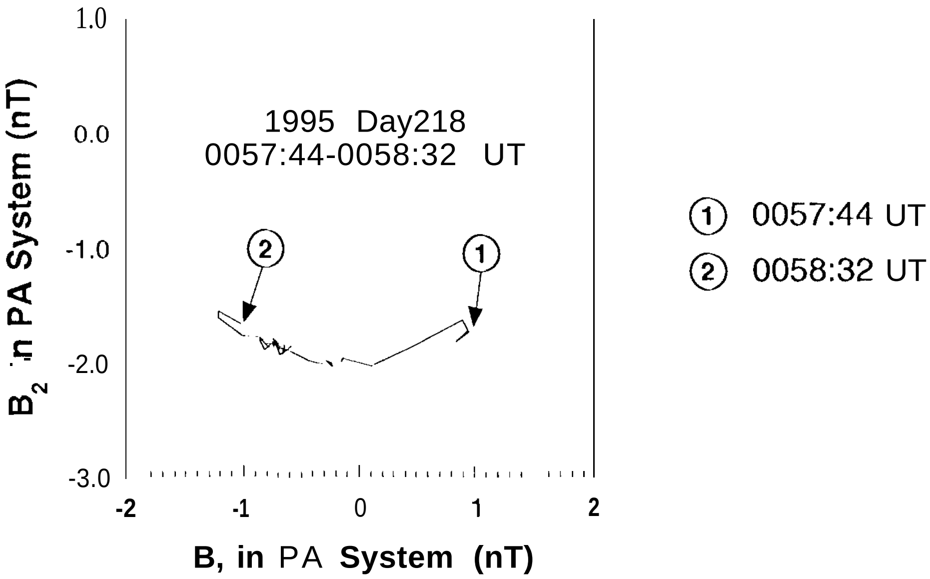

Figure 1

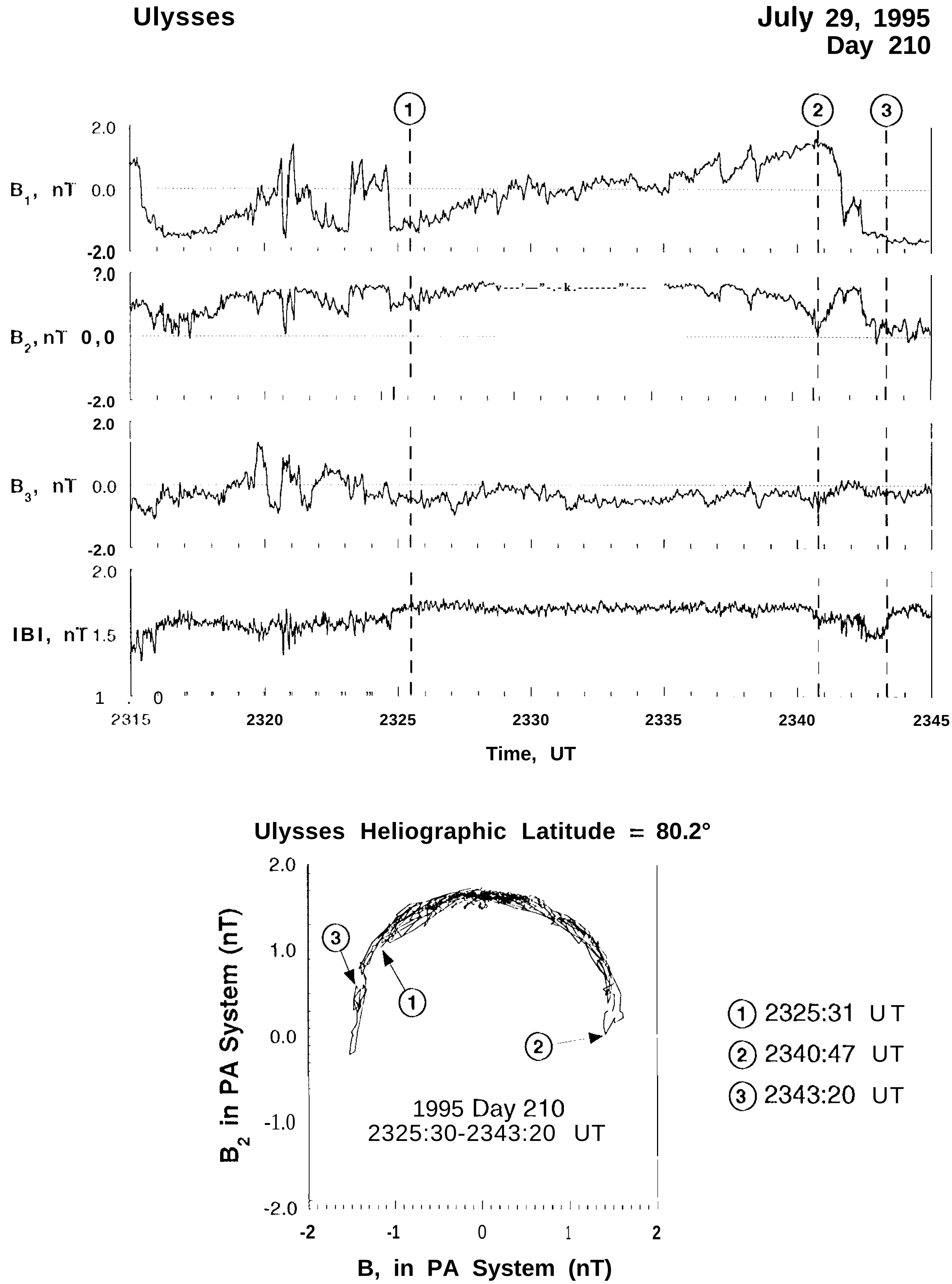
Ulysses
July 29, 1995
Day 210
B1, nT
B2, nT
B3, nT
IBI, nT
Time, UT
Ulysses Heliographic Latitude = 80.2°
B2 in PA System (nT)
B, in PA System (nT)
1995 Day 210
2325:30-2343:20 UT
1 2325:31 UT
2 2340:47 UT
3 2343:20 UT

Figure 2

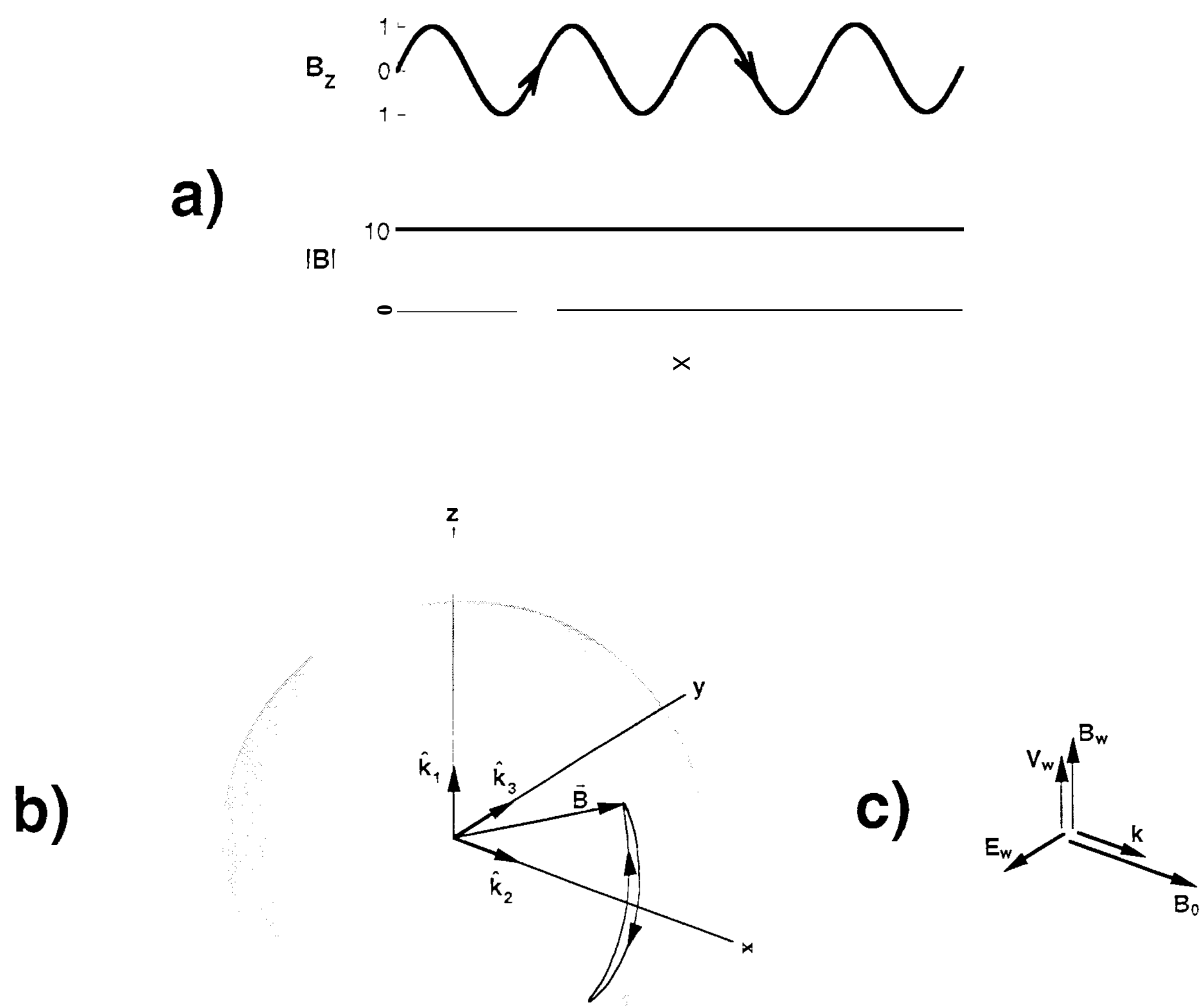

Figure 3

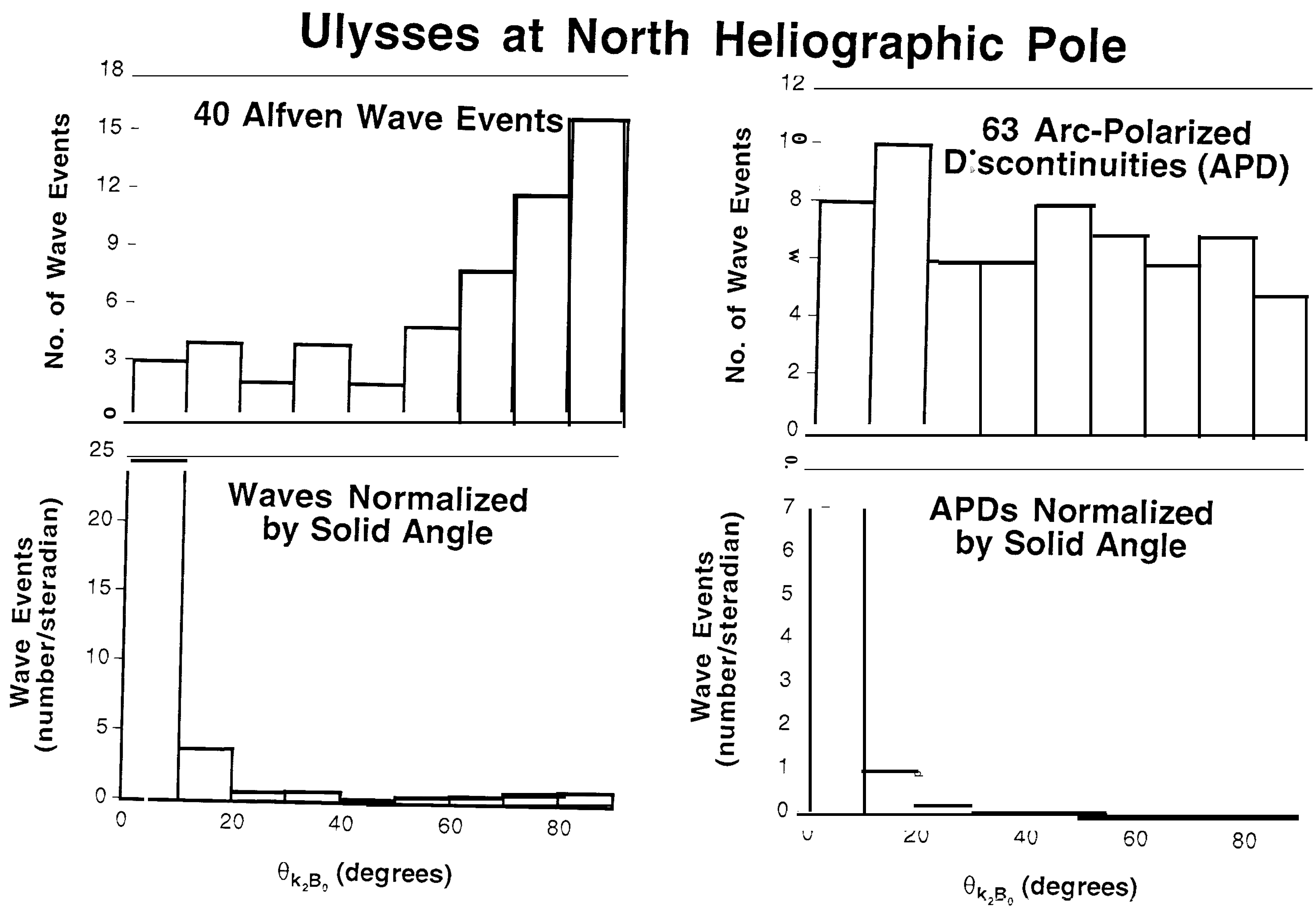
Ulysses at North Heliographic Pole
40 Alfven Wave Events
No. of Wave Events
18
15
12
9
6
3
0
63 Arc-Polarized Discontinuities (APD)
12
10
8
4
2
0
Waves Normalized by Solid Angle
Wave Events (number/steradian)
25
20
15
10
5
0
20
40
60
80
$\theta_{k_2B_0}$ (degrees)
APDs Normalized by Solid Angle
7
6
5
4
3
2
1
0
20
40
60
80
$\theta_{k_2B_0}$ (degrees)

Figure 4